Topological Nodal-Point Superconductivity in Two-Dimensional Ferroelectric Hybrid Perovskites

Xiaoyin Li[1], Shunhong Zhang[2], Xiaoming Zhang[3], Zeev Valy Vardeny[4], Feng Liu[1]*
[1]Department of Materials Science and Engineering, University of Utah, Salt Lake City, Utah 84112, United States
[2]International Center for Quantum Design of Functional Materials, University of Science and Technology of China, Hefei, Anhui 230026, China
[3]College of Physics and Optoelectronic Engineering, Ocean University of China, Qingdao, Shandong 266100, China
[4]Department of Physics & Astronomy, University of Utah, Salt Lake City, Utah 84112, United States
*e-mail: fliu@eng.utah.edu

INTRODUCTION

Topological superconductors (TSCs) are of great interest for hosting Majorana modes, which are non-Abelian quasiparticles promising for fault-tolerant quantum computing. While intrinsic TSCs are rare, extrinsic TSCs can be obtained in heterostructures by combining conventional superconductors with materials exhibiting spin-momentum locking, such as Rashba spin-orbit coupling (SOC) semiconductors [1, 2]. Although several candidate materials have been proposed, experimental realization remains challenging due to difficulties in synthesizing materials with suitable thickness and orientation, fabricating high-quality interfaces, and the typically small nontrivial superconducting gap, which hinders the detection of Majorana modes.

OBJECTIVE

This work [3] aims to identify new material candidates that overcome the challenges above. We find that two-dimensional (2D) hybrid organic-inorganic perovskites (HOIPs) offer promising features, such as structural diversity, strong SOC, and weak van der Waals interactions, for realizing TSC. Motivated by these advantages, we explore the potential of TSC in 2D HOIPs, focusing on utilizing the previously unexplored anisotropic SOC present in ferroelectric 2D HOIPs.

RESULTS

Figure 1 compares isotropic Rashba SOC and anisotropic SOC, along with their realized topological superconducting (TSC) and nodal-point superconducting (NSC) phases after including s-wave superconducting pairing and Zeeman splitting. Isotropic SOC leads to a fully gapped TSC with Majorana modes on all sample edges, while anisotropic SOC results in NSC with topologically protected nodal points and Majorana modes on specific edges. Using first-principles calculations (Fig. 2) and tight-binding modelling (Fig. 3) on a specific material with room-temperature ferroelectricity, BA_2PbCl_4 (BA = benzylammonium), we demonstrate the emergence of NSC and Majorana edge modes in 2D HOIPs. Furthermore, the intrinsic ferroelectricity of such 2D HOIPs offers additional tunability, enabling control of NSC phases and Majorana modes at ferroelectric domain walls as well as edges (Fig. 4).

CONCLUSION

We proposed and demonstrated 2D ferroelectric HOIPs as promising candidates to realize NSC and gapless Majorana modes, waiting for experimental realization. Also, NSC is protected by spatial symmetries of 2D HOIPs, therefore more exotic topological superconducting states could be found in this class of materials.

REFERENCES

[1] J. D. Sau, R. M. Lutchyn, S. Tewari, S. Das Sarma, Phys. Rev. Lett. **104**, 040502 (2010).
[2] R. M. Lutchyn, J. D. Sau, S. Das Sarma, Phys. Rev. Lett. **105**, 077001 (2010).
[3] X. Li, S. Zhang, X. Zhang, Z. V. Vardeny, F. Liu, Nano Lett. **24**, 2705-2711 (2024).

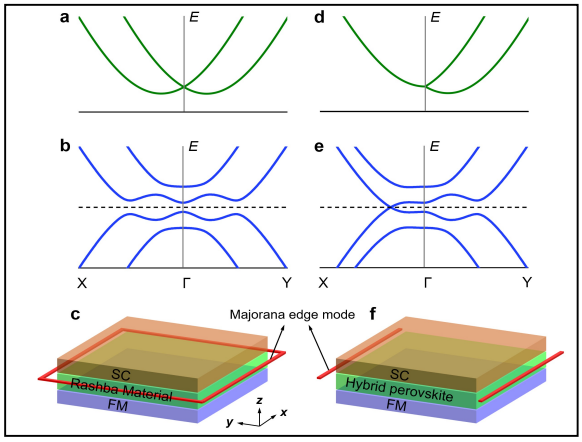

Fig. 1. Schematics of topological superconductivity (TSC) vs topological nodal-point superconductivity (NSC) based on non-centrosymmetric semiconductors with isotropic vs anisotropic SOC. Isotropic SOC: (a) The SOC-related split electronic band structure. (b) BdG quasiparticle band structure. (c) The Majorana edge mode. Anisotropic SOC: (d)-(f) Same as in (a)-(c) but for the two-dimensional hybrid organic-inorganic perovskite with anisotropic SOC.

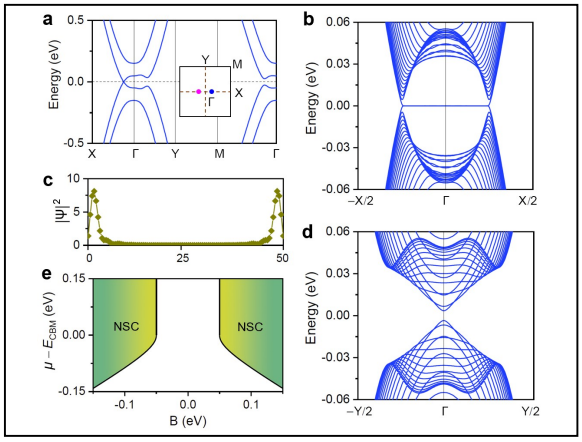

Fig. 3. NSC in BA_2PbCl_4 monolayer. (a) BdG quasiparticle band structure along high-symmetric k paths. Inset plots two nodal points in the Brillouin zone, whose chirality is shown by different colors (purple/blue for +/−). (b) and (c) BdG band structure of a nanoribbon terminated along y-direction and real-space distributions of emerged gapless Majorana modes. (d) BdG band structure of a nanoribbon terminated along x-direction. (e) NSC phase diagram in the parameter space of chemical potential μ and Zeeman field B with a fixed $\Delta = 0.05$ eV. For (a)-(d), $\mu = 1.23$ and $B = 0.1$ eV. The widths of the two nanoribbons are both 50 unit-cells.

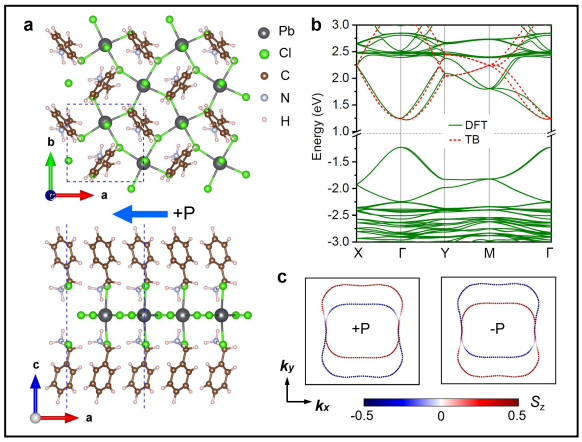

Fig. 2. Atomic and electronic structure of the ferroelectric BA_2PbCl_4 monolayer. (a) Top and side views of atomic structure. The blue arrow (+**P**) indicates the direction of ferroelectric polarization. (b) Electronic band structure along high-symmetric k paths of the Brillouin zone. (c) Conduction band energy contours (E = 1.58 eV) of the BA_2PbCl_4 monolayer with opposite polarization direction (+**P** and −**P**). The S_z component of spin is mapped by the color bar, while the S_x and S_y components are constrained to zero by crystal symmetry.

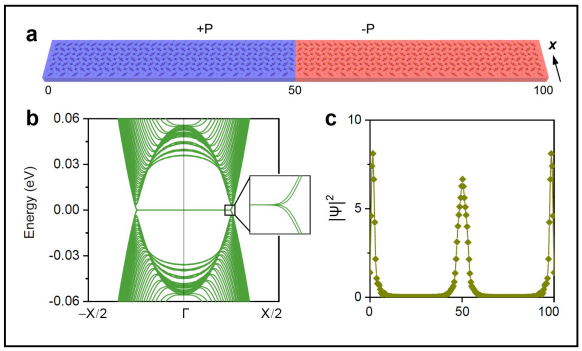

Fig. 4. Domain-wall Majorana modes in the BA_2PbCl_4 monolayer. (a) Illustration of ferroelectric two-domain structure, which is terminated along y-direction and periodic along x-direction. The widths of the left and right domains are both 50 unit-cells. (b) BdG band structure of the two-domain structure proximate to an s-wave SC ($\Delta = 0.05$ eV) and a FM with y-direction magnetization (B = 0.1 eV), showing the emergence of four gapless Majorana modes. (c) Real-space distributions of the four Majorana modes, peaking at the outer edges as well as the inner domain wall.